Neuron, Vol. 42, 77–88, April 8, 2004, Copyright ©2004 by Cell Press

Afferent Induction of Olfactory Glomeruli Requires N-Cadherin

Thomas Hummel[1,2] and S. Lawrence Zipursky[1,*]
[1]Howard Hughes Medical Institute
Department of Biological Chemistry
Geffen School of Medicine
Molecular Biology Institute
Box 951662
University of California, Los Angeles
Los Angeles, California 90095
[2]Institut fuer Neurobiologie
Universitaet Muenster
Badestrasse 9
D-48149 Muenster
Germany

Summary

Drosophila **olfactory receptor neurons (ORNs) elaborate a precise internal representation of the external olfactory world in the antennal lobe (AL), a structure analagous to the vertebrate olfactory bulb. ORNs expressing the same odorant receptor innervate common targets in a highly organized neuropilar structure inside the AL, the glomerulus. During normal development, ORNs target to specific regions of the AL and segregate into subclass-specific aggregates called protoglomeruli prior to extensive intermingling with target dendrites to form mature glomeruli. Using a panel of ORN subclass-specific markers, we demonstrate that in the adult AL, *N-cadherin (N-cad)* mutant ORN terminals remain segregated from dendrites of target neurons. N-cad plays a crucial role in protoglomerulus formation but is largely dispensible for targeting to the appropriate region of the AL. We propose that N-cad, a homophilic cell adhesion molecule, acts in a permissive fashion to promote subclass-specific sorting of ORN axon terminals into protoglomeruli.**

Introduction

Sensory neurons convert external stimuli into internal neural representations. In the vertebrate visual system, for instance, retinal ganglion cell axons form continuous topographic maps in which their relative spatial relationships in the eye are conserved in the pattern of synaptic connections in the tectum or superior colliculus (Goodhill and Richards, 1999). The formation of such retinotopic maps relies on the graded expression of Ephrins and their receptors, Ephs, in growth cones and their targets (Wilkinson, 2000). By contrast, in mouse and *Drosophila*, olfactory receptor neurons (ORNs) elaborate discontinuous spatial maps in which ORNs expressing the same odorant receptor, distributed over the surface of the sense organ, form connections to a common set of CNS dendrites spatially segregated into a structure called a glomerulus (Gao et al., 2000; Mombaerts et al., 1996; Vosshall et al., 2000; Wang et al., 1998). As each ORN expresses one of a large number of different odorant receptors, a map of odor quality or identity emerges through the targeting of ORNs expressing the same odorant receptor to one or a small number of glomeruli (Ressler et al., 1994; Sullivan et al., 1995). The glomerulus is an evolutionarily conserved neural processing unit containing ORN axons and dendrites of target neurons (Hildebrand and Shepherd, 1997; Strausfeld and Hildebrand, 1999). In the mouse, odorant receptors play an instructive role in targeting of ORNs to specific glomeruli (Mombaerts et al., 1996; Wang et al., 1998). Despite the similarity in the overall structure of the fly and mouse olfactory systems, targeting of fly ORNs seems to be independent of odorant receptors (Dobritsa et al., 2003; Elmore et al., 2003; Elmore and Smith, 2001).

In *Drosophila*, some 1500 ORNs in the antenna and the maxillary palps send axons into the antennal lobe (AL), where they form connections in 40–50 glomeruli (Laissue et al., 1999). Each glomerulus contains dendritic processes of projection neurons (PNs) and local interneurons (LNs) (Stocker, 1994; Stocker et al., 1990). PN identity is determined prior to the arrival of ORN axons into the AL (Jefferis et al., 2001; Komiyama et al., 2003), and many PN dendrites elaborate distinct patterns in the target field prior to ORN innervation (Jefferis et al., 2004). In turn, ORNs may target to specific regions of the AL based on selective recognition of different PN dendrites. Alternatively, initial ORN targeting may rely on PN-independent cues. Matching ORN and PN dendrites in close proximity may then initiate a program of cellular interactions leading to glomerulus formation. In addition to the obvious importance of PN/ORN interactions in forming connections, studies in both vertebrates and invertebrates suggest that ORN/ORN interactions play a crucial early role in glomerulus formation (Ebrahimi and Chess, 2000; Kent et al., 1999; Oland and Tolbert, 1996; Royal et al., 2002; Valverde et al., 1992; Vassalli et al., 2002). During normal development, ORNs form so-called protoglomeruli that comprise processes of ORN axons largely devoid of target dendrites (Oland et al., 1990; Potter et al., 2001; Treloar et al., 1999). Indeed, ORNs deprived of their normal targets form ectopic glomerular-like structures (Goheen et al., 1995; Graziadei and Kaplan, 1980; Graziadei and Monti Graziadei, 1986; Oland and Tolbert, 1998; Rossler et al., 1999; St John et al., 2003). In summary, the connections between ORNs and their targets requires prepatterning of the AL neuropil by PN dendrites, ORN/ORN interactions, and interactions between ORNs and target dendrites.

We previously demonstrated that Dscam, a member of the Ig domain superfamily, plays a crucial role in determining target specificity for a subclass of ORNs in *Drosophila* (Hummel et al., 2003). *Dscam* mutant ORNs frequently terminate in inappropriate locations. Interestingly, at these ectopic target sites, *Dscam* mutant ORNs are not intermingled with axons from other ORN classes but still sort out from them and converge in a subclass-specific manner. These observations underscore the no-

*Correspondence: zipursky@hhmi.ucla.edu

tion that target cell-independent mechanisms selectively promote adhesion between ORN growth cones expressing the same odorant receptors. Indeed, studies in the vertebrate olfactory system support specific adhesive interactions between ORNs expressing the same odorant receptor and, furthermore, that odorant receptors contribute to sorting specificity (Vassalli et al., 2002; see Discussion). The molecules regulating sorting of fly ORNs remain unknown, but they are unlikely to include odorant receptors based on gain- and loss-of-function genetic studies (Dobritsa et al., 2003).

To uncover the molecular basis of wiring specificity in the olfactory system, we have initiated both forward genetic screens and candidate gene approaches for ORN targeting mutants. In this paper, we present evidence that N-cadherin (N-cad), a classical cadherin that mediates calcium-dependent homophilic cell adhesion (Iwai et al., 1997), plays a crucial role at a discrete step in ORN targeting. ORN subclasses lacking N-cad project to the appropriate region of the AL but do not form protoglomeruli and remain segregated from target dendrites. We propose that N-cad acts in combination with additional specificity factors to promote selective association of ORN growth cones expressing the same odorant receptors in the target field.

Results

N-cad Mutant ORNs Fail to Innervate the AL Dendritic Field

To assess the importance of N-cad in ORN targeting, we generated mosaic flies with *N-cad* mutant ORNs and a heterozygous (i.e., wild-type) AL target. Cells in the antenna were rendered homozygous mutant for a null allele of *N-cad* using the MARCM system (Lee and Luo, 1999). *eyeless-Flp* (*eyFLP*) (Newsome et al., 2000; Stowers and Schwarz, 1999) was used to induce mitotic recombination in ORN progenitor cells, but not their target neurons (Hummel et al., 2003). All mutant ORNs were visualized using elav-Gal4 to drive expression of UAS-mCD8-GFP (Figure 1). Four different strong loss-of-function *N-cad* alleles (see Experimental Procedures) exhibited indistinguishable phenotypes and were fully penetrant ($n > 30$ brains/genotype).

In the adult, wild-type ORNs project from the antennal nerve into the nerve fiber layer (NFL) surrounding the AL neuropil (Figures 1A and 1B–1D). Branches from these axons project into specific glomeruli in the ipsilateral AL and ramify throughout them. Axons continue to extend across the AL to a mirror symmetric contralateral glomerulus. The general neuropil marker nc82 highlights the compact glomerular organization of the AL neuropil (Figure 1C). As in wild-type, *N-cad* mutant ORN axons reached the AL, projected along the periphery in the NFL, and extended normally through the commissure to the contralateral lobe (Figures 1E and 1G; see also Figure 3). In marked contrast to wild-type, however, *N-cad* mutant ORN axon terminals remained largely on the surface of the AL (Figures 1E and 1G). Indeed, only a few ORN fibers penetrated the AL neuropil (arrows in Figure 1E). Defects in AL organization were also visible using the nc82 marker (Figures 1C and 1F). ALs into which *N-cad* mutant ORNs projected showed a marked disorganization of glomerular structure (Figures 1C, 1D, 1F, and 1G); in most regions of the AL, subdivision of the neuropil into glomeruli was not evident. In summary, ORNs require N-cad for innervating the AL neuropil and for the formation of glomeruli.

N-cad Mutant ORN Subclasses Target to the Appropriate Regions of the AL

To analyze axonal targeting of *N-cad* mutant ORNs, we visualized their connectivity pattern using a set of ORN subclass-specific markers. To this end, different odorant receptor promoters were fused to Gal4 that, in turn, activate expression of UAS-CD8-GFP or a presynaptic marker, UAS-N-synaptobrevin-GFP (Figure 2). Ten different subclasses of ORNs were tested, including seven from the antenna (Or22a, Or23a, Or47a, Or47b, GH298, and two subclasses that express the enhancer trap marker 72OK, see Figure 7) and three that project from the maxillary palps (Or46a, Or59c, and Or71a). *N-cad* mutant ORNs were generated and selectively labeled using *eyFLP* and the MARCM system.

All subclasses of ORNs exhibited a similar axonal phenotype (Figures 2A–2V; data not shown). *N-cad* mutant axons typically targeted to the appropriate region of the AL but failed to converge on a single glomerulus. This is particularly clear for Or46a (Figures 2A–2C) and, to a lesser extent, for Or47b (Figures 2D–2F). The localization of ORN axons to the surface of the AL is highlighted by the examples for Or22a (Figures 2G–2I) and Or59c (Figures 2J–2L). These fibers accumulated on the medial surface of each AL. Although the phenotype of mutant Or46a axons is similar to other ORN classes, it is more severe. Mutant Or46a axons seldom converge close to their targets, in contrast to most ORN subclasses where at least a fraction accumulate in a region of the AL corresponding to their glomerular targets in wild-type. Interestingly, the severity of the phenotype is similar to Or71a mutant axons (data not shown), a different ORN subclass projecting from the maxillary palps and terminating, like Or46a, on the anterior face of the AL. This does not reflect a difference in requirements for maxillary palp ORNs, since Or59c, another maxillary palp ORN that targets to the medial surface of the lobe, has a phenotype similar to the antennal ORN, Or22a. Hence, the discrepancies in phenotypes may reflect different requirements for N-cad for targeting to different regions of the AL or the variable contributions of redundant mechanisms in different ORN subclasses.

While most glomeruli in *N-cad* mosaics were not visible using the neuropil marker nc82, there were several prominent exceptions (Figures 2M–2R). These included the glomeruli innervated by the ORN subclasses GH298 and Or47a. Despite the retention of glomerular structure, *N-cad* mutant ORNs remained at the surface of these glomeruli and did not penetrate them. This is particularly evident for *N-cad* mutant GH298 axons that lie on the ventral surface of the V glomerulus (Figures 2M–2O). These weaker phenotypes may reflect redundant mechanisms (e.g., the contribution of other cadherin-like molecules) or an increased fraction of wild-type ORNs in these less affected subclasses (see Ebrahimi and Chess, 2000).

To assess whether the presence of wild-type ORNs

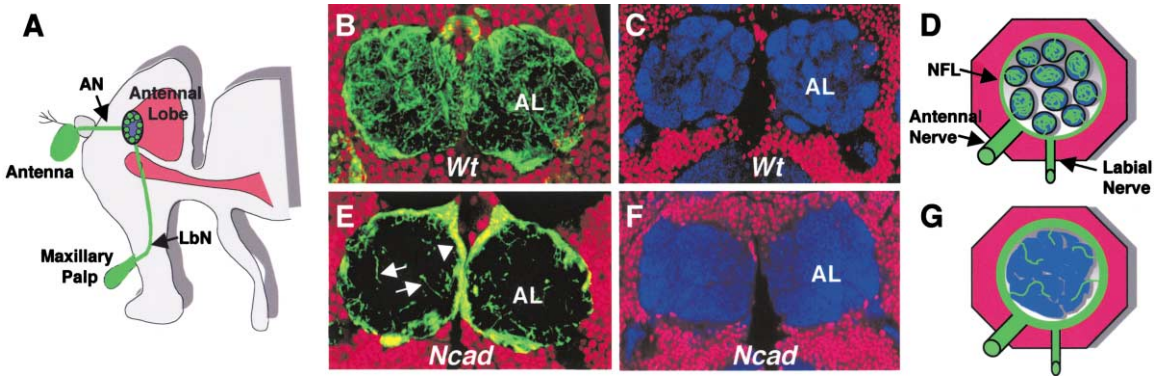

Figure 1. Removal of *N-cad* from ORNs Disrupts the Structure of Glomeruli in the Antennal Lobe

(A and D) Schematic representations of the *Drosophila* olfactory system. (A) Olfactory receptor neurons (ORNs) project axons from the antenna and maxillary palp into the antennal lobes (AL) through the antennal nerve (AN) or labial nerve (LbN), respectively. (D) ORNs course through the nerve fiber layer (NFL) surrounding the AL neuropil. An individual ORN elaborates highly branched thin processes into a single target glomerulus (see Figure 2).

(B) Wild-type ORN axons were labeled by elav-Gal4 driven CD8-GFP (green) and the MARCM method. ORNs extend processes throughout the AL.

(C) The neuropil in the AL is organized into glomerular units, visualized by the mAb nc82 (blue). Identity of individual glomeruli can be determined by their shape and relative position.

(D) Schematic representation summarizes organization of the AL (see above).

(E) *N-cad* mutant ORN axons reach the AL and project along the periphery. Only a few isolated ORN axons were seen within the AL neuropil (arrows). ORN processes largely remain in the NFL (arrowhead).

(F) Severe disruption of the glomerular organization of the AL neuropil is seen in mosaic animals in which ORNs are *N-cad* mutant and the target cells in the AL are wild-type. As shown here, no glomerular subdivision was detected at the anterior surface of the AL.

(G) Schematic representation of (E) and (F) illustrates the peripheral location of ORN axons within a thickened NFL and loss of glomerular structure seen in ALs of mosaic animals with *N-cad* mutant ORNs and a wild-type target.

Neuronal nuclei (red) are labeled with anti-elav (B and E) and TOTO-3 (C and F). Genotypes: (B and C) *eyFLP; FRT40/Gal80 FRT40; elav-Gal4 UAS-mCD8GFP*; (E and F) *eyFLP; N-cad FRT40/Gal80 FRT40; elav-Gal4 UAS-mCD8GFP*.

innervating a given glomerulus may mitigate the severity of the glomerular defects, we increased the fraction of mutant ORNs in mosaic animals by selecting against cells carrying two wild-type *N-cad* alleles using a *cycE* mutation (see Experimental Procedures). In these animals, glomeruli, which were still recognizable in MARCM clones, largely disappeared. For instance, the DM3 glomerulus innervated by Or47a was missing and, although the V glomerulus innervated by GH298 remained visible, it appeared reduced in size (data not shown). This increase in phenotypic strength was also seen with Or47a neurons marked with synaptobrevin-GFP. Terminals of *N-cad* mutant Or47a neurons were no longer restricted to the appropriate target region in the dorsomedial region of the AL but extended into the adjacent commissure (compare Figures 2Q and 2S). By contrast, the axonal phenotypes of most ORN subclasses (Or22a, Or46a, Or47b, Or59c, and Or71a) were largely the same in mosaics generated in a *cycE* and wild-type background, as shown for Or22a in Figures 2U and 2V.

To assess whether *N-cad* mutant ORNs extended branches to the contralateral side, one antenna was removed to promote the degeneration of ipsilateral projections and the projections of the Or22a subclass were assessed (Figures 3A and 3B). This revealed that axons branched as in wild-type and extended processes to the contralateral side. These axons largely targeted to the correct region of the AL but also remained separate, lying above the neuropil and spreading into neighboring ventral AL regions (Figure 3B, arrows). The failure of *N-cad* mutant ORNs to invade their cognate glomeruli is a cell-autonomous function, as it was also seen for single mutant Or22a axons in an otherwise wild-type background (Figures 3C and 3D). Single-cell analysis also revealed that single mutant Or22a fibers projected to the appropriate region of the ipsi- and contralateral ALs. That these phenotypes reflect loss of *N-cad* only was supported by the finding that all four *N-cad* alleles tested showed similar phenotypes and that defects were rescued by expression of an N-cad cDNA transgene specifically in homozygous mutant ORNs (Figures 3E and 3F). In a similar rescue experiment, overall glomerular organization, as well as ORN innervation throughout the AL, was restored by the expression of single N-cad cDNA in all mutant ORNs (data not shown). While alternative splicing at the *N-cad* locus can give rise to eight different forms of N-cad (S. Hsu, H. Robertson, and A. Chiba, personal communication), a single form appeared to be sufficient for its function in ORNs.

In summary, these data establish that N-cad is not required in ORNs for targeting to specific regions of the AL, but it mediates the ORN subclass-specific convergence of axon terminals in the AL dendritic field.

N-cad Mutant ORN Terminals Segregate from PN and LN Dendrites

We set out to assess whether lack of N-cad in ORN axons disrupted the organization of PN and LN dendrites. LNs and PNs form characteristic patterns within glomeruli and occupy distinct glomerular subcompartments (Figures 4A–4D and 5A–5C). The dendrites from a single LN typically ramify throughout each AL. Only a few LN dendrites protrude into a given glomerulus (e.g., DM2; Figures 4A–4D). These have thick profiles and are

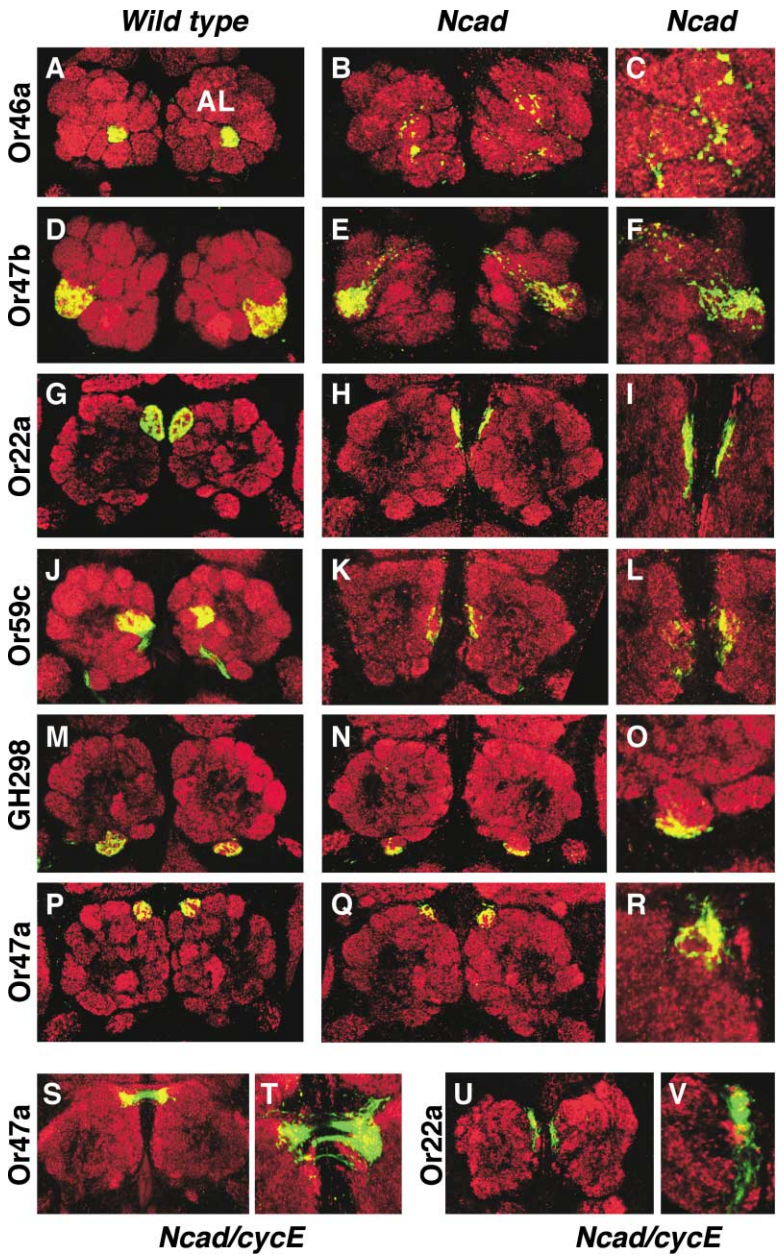

Figure 2. *N-cad* Mutant ORN Axons Project to the Right Region of the AL but Remain at the Surface of the Neuropil

Targeting of different ORN classes was visualized by expressing UAS-synaptobrevin-GFP under the control of OR-Gal4 driver lines (green). The AL neuropil is labeled with the mAb nc82 (red). The overlap between the two markers is yellow. Different ORN classes (Or46a, Or47b, Or22a, Or59c, GH298, and Or47a) are shown in wild-type (A, D, G, J, M, and P) and *N-cad* mutant clones (B, C, E, F, H, I, K, L, N, O, Q–V). Wild-type ORNs expressing the same odorant receptor project into the same glomerulus.

(A–C) Wild-type (A) and *N-cad* mutant (B and C) Or46a projections. *N-cad* mutant axon terminals spread out over the surface of the anterior central region of the AL.

(D–F) Wild-type (D) and *N-cad* mutant (E and F) Or47b projections. Some mutant terminals converge on their appropriate glomeruli while others spread out over the anterior surface of the AL.

(G–I) Wild-type (G) and *N-cad* mutant (H and I) Or22a projections. *N-cad* mutant terminals spread out over the posterior medial surface of the lobe.

(J–L) Wild-type (J) and mutant (K and L) Or59c projections. Mutant terminals also spread out over the posterior medial surface of the lobe just ventral to Or22a.

(M–O) GH298 projections. Mutant terminals target to the appropriate glomerulus but do not enter it.

(P–T) Wild-type (P) and mutant (Q–T) Or47a projections.

(R) Mutant terminals lie on the surface of the appropriate glomerulus.

(S and T) By increasing the fraction of Or47a axons that are *N-cad* mutant, the DM3 glomerulus structure is lost (T) and fibers extend past the dorsal medial region of the lobe and into the adjacent commissure (S and T) (see text).

(U and V) Increasing the fraction of *N-cad* mutant ORNs using a *cycE* mutation does not increase the strength of the phenotype for Or22a (and most other ORN subclasses) when compared to mosaics using a wild-type chromosome (compare with the phenotypes for 22a in G–I).

Genotypes: (A, D, G, J, M, P) *eyFLP*; *FRT40/Gal80 FRT40; Or-Gal4 UAS-sybGFP*; remaining panels (except S–V) *eyFLP; N-cad FRT40/Gal80 FRT40; Or-Gal4 UAS-sybGFP*; (S–V) *eyFLP; N-cad FRT40/cycE FRT40; Or-Gal4 UAS-sybGFP*.

surrounded by ORN processes. Conversely, most PNs extend dendrites into a single glomerulus. These dendrites are finer in appearance and course throughout the glomerulus, revealing extensive overlap with ORN processes (Figures 5A–5C). To assess the relationship between wild-type LNs and mutant ORN terminals, we visualized both cell types in mosaic animals in which *N-cad* mutant ORNs projected into a wild-type AL (Figures 4E–4H). The Or22a axon terminals were highlighted using synaptobrevin-GFP and the LN dendrites by GH298-driven expression of LacZ. *N-cad* mutant Or22a axons were found at the medial surface of the AL segregated from LN dendrites. Similar experiments were done using synaptobrevin-GFP-labeled *N-cad* mutant ORNs and LacZ-labeled PN dendrites (under the control of GH146-Gal4). For reasons that remain unclear, while controls stained strongly for LacZ (Figure 5A), mosaic ALs stained poorly. As such, we were unable to critically assess the spatial relationship between identified PN dendrites and ORN terminals. However, as N-cad itself is expressed in PNs, as well as other processes within the neuropil, we analyzed mosaic animals double-stained with anti-N-cad and Or22a-sybGFP (N.B., Or22a mutant axons do not stain with anti-N-cad). No overlap

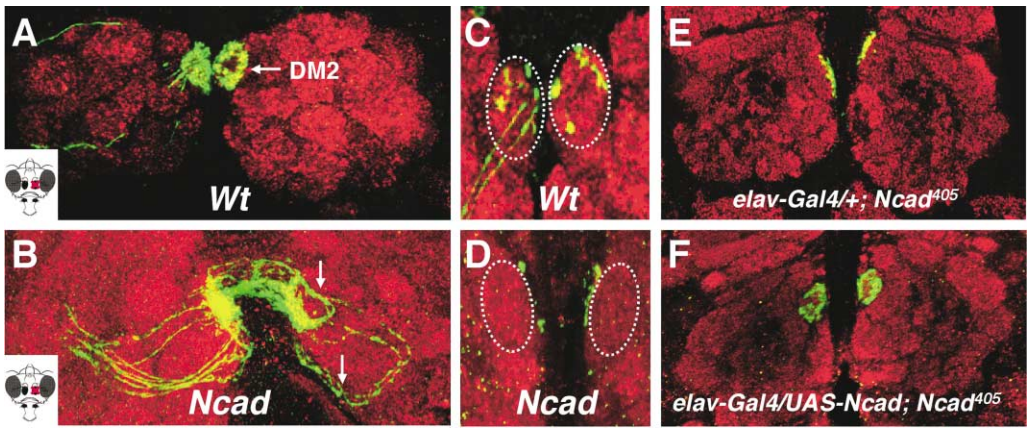

Figure 3. Phenotypic Characterization of *N-cad* Mutant Or22a Axons

(A and B) Or22a axons project to both the ipsilateral and contralateral DM2 glomerulus in the dorsal AL. (A) Wild-type Or22a axons project to the ipsilateral side and send a branch contralaterally to the same glomerulus. The contralateral projections can be visualized by removing the contralateral antenna. As in wild-type, *N-cad* mutant ORNs (B) send branches to the contralateral side, but mutant axon terminals spread out into neighboring AL regions (arrows). The icons in the lower left in (A) and (B) indicate which antennae were removed.

(C and D) The projection phenotype of single wild-type and *N-cad* mutant Or22a fibers in an otherwise wild-type background. (C) Innervation of two wild-ype Or22a axons on the ipsi- and contralateral DM2 glomerulus (single confocal section). (D) Single *N-cad* mutant Or22a axons do not invade the glomerular neuropil and instead lie at the surface (merged image shows no evidence of fibers within the glomerulus). The single *N-cad* mutant fiber also extends to the contralateral side where it terminated near, but not within, the DM2 glomerulus (circular dashed lines).

(E and F) The *N-cad* mutant phenotype of Or22a (E) in genetically mosaic animals with mutant ORNs and a wild-type target (F). This phenotype was rescued by expression of *N-cad* in mutant ORNs.

Genotypes: (A) *eyFLP*; *FRT40/Gal80 FRT40; Or22a-Gal4 UAS-mCD8GFP*; (B) *eyFLP*; *N-cad FRT40/Gal80 FRT40; Or22a-Gal4 UAS-mCD8GFP*; (C) *hs-Flp*; *FRT40/Gal80 FRT40; Or22a-Gal4 UAS-mCD8GFP*; (D) *hs-Flp*; *N-cad FRT40/Gal80 FRT40; Or22a-Gal4 UAS-mCD8GFP*; (E) *eyFLP elav-Gal4/+ ; Or22a-sybGFP N-cad FRT40/Gal80 FRT40*; (F) *eyFLP elav-Gal4/ UAS-N-cad ; Or22a-sybGFP N-cad FRT40/Gal80 FRT40*.

between N-cad-staining dendritic processes and *N-cad* mutant Or22a axons was observed (Figures 5D and 5E).

PN and LN dendrites in mosaic animals with *N-cad* mutant ORNs retained many morphological features characteristic of these cells innervated by wild-type ORNs (Figures 4A and 4E and Figures 5F and 5K). LNs,

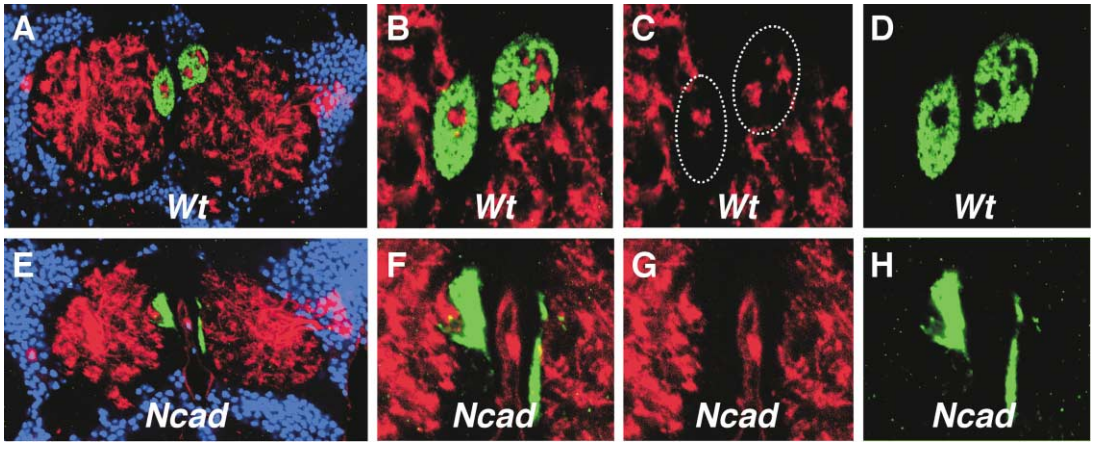

Figure 4. The Spatial Relationship between ORN Axon Terminals and LN Dendrites Requires N-Cad in ORNs

The morphology of LNs in the ALs of wild-type animals (A–D) and after removing *N-cad* from ORNs (E–H). LNs and Or22a axons are in red and green, respectively.

(A–D) In wild-type, LNs send their dendrites into multiple glomeruli (A), but their terminal branches occupy only a small region in the central part of each glomerulus (B and C). Terminal branches of LN dendrites in the center of DM2 are surrounded by ORN 22a synaptic terminals (B and D).

(E–H) In ALs receiving *N-cad* mutant ORNs (E), LNs elaborate extensive dendritic fields as in ALs innervated by wild-type ORNs. Rather than surrounding LN dendrites, *N-cad* mutant ORNs remain separate from LN dendrites on the surface of the AL (F–H).

(A and E) TOTO-3 nuclear staining is shown in blue. (B, D, F, and H) Synaptobrevin-GFP expression driven by OR22a is shown in green. (A–C, E–G) LacZ expression under the control of a GH298 is shown in red. GH298 is expressed in ORNs innervating the V glomerulus (see Figure 2) and in LNs. The staining of LNs is not seen in the analyses of targeting of GH298 ORNs in Figure 2 as it is suppressed by Gal80. Genotypes: (A–D) *eyFLP; Or22a-sybGFP FRT40/cycE FRT40; GH298-Gal4 UAS-LacZ*; (E–H) *eyFLP; Or22a-sybGFP N-cad FRT40/cycE FRT40; GH298-Ga4 UAS-LacZ*.

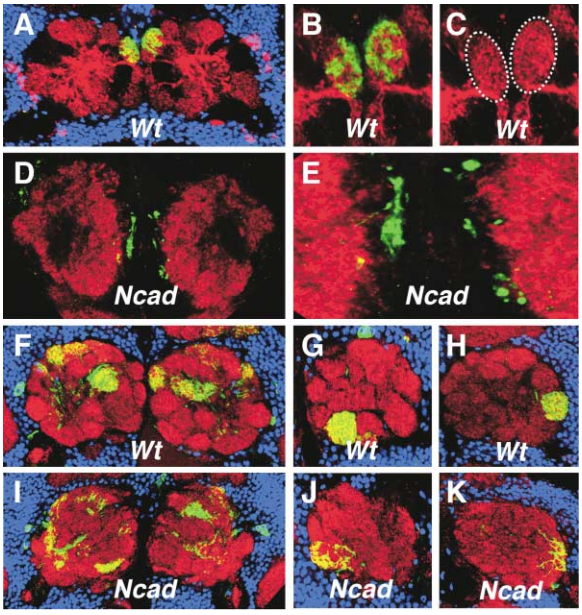

Figure 5. *N-cad* Mutant ORN Terminals Do Not Overlap with Wild-Type PN Dendrites and Disrupt PN Dendritic Arbor Morphology

(A–C) Innervation of glomeruli by PN dendrites in wild-type. In contrast to LNs, the dendrites of the PNs (a subset of which are labeled with the GH146 marker) extend throughout the whole DM2 glomerulus (outline of dashed lines in C), overlapping extensively with ORN terminals.

(D and E) *N-cad* mutant Or22a axon terminals do not contact the postsynaptic target field. For unknown reasons, the GH146 marker was very weak in PNs after removing N-cad from ORNs (data not shown). Hence, the postsynaptic neuropil was labeled here with anti-N-cad antibody (red). As N-cad is not expressed in *N-cad* mutant ORNs, this provides a convenient marker.

(F–K) PN dendritic patterns were disrupted by *N-cad* mutant ORNs. (F–H) Wild-type PN dendritic fields are largely uniglomerular (in F multiple cells were labeled, whereas single cells were labeled in G and H). Typically dendritic fields are spherical. (I–K) In contrast, wild-type PN dendrites in a *N-cad* ORN mutant background appeared flattened and more dispersed. A small number of labeled PNs is shown in (I) with single mutant clones shown in (J) and (K).

TOTO-3 nuclear staining is shown in blue (A, F–K). Synaptobrevin-GFP expression driven by OR22a is shown in green and GH146 Gal4 driving UAS-lacZ is in red (A–C). Anti-N-cad (D and E) and neuropil marker mAb nc82 (F–K). Genotypes: (A–C) *eyflp; GH146-Gal4 FRT40/cycE FRT40; OR22a-sybGFP UAS-lacZ*; (D and E) *eyflp;OR22a-sybGFP N-cad FRT40/cycE FRT40*; (F–H) *eyflp/hsflp; GH146-Gal4 FRT40/cycE FRT40; UAS>CD2>CD8-GFP*; (I–K) *eyflp/hsflp; GH146-Gal4 N-cad FRT40/cycE FRT40; UAS>CD2>CD8-GFP*.

for instance, coursed broadly thoughout the neuropil with thickened terminal branches (Figures 4A and 4E). Similarly, PN dendrites (Figures 5F–5K) extended processes in localized regions of the AL. In contrast to wild-type, however, PN dendrites in mosaics frequently elaborated highly irregular shapes (Figures 5I–5K). In wild-type, PN dendrites appeared as densely stained structures with precisely defined smooth, often-rounded borders (Figures 5F–5H). By contrast, PN dendrites in mosaics had poorly defined borders, extended through larger regions of the lobe, and intermingled with PN dendrites that in wild-type animals innervate different glomeruli (Figures 5I–5K and data not shown).

In summary, N-cad is required in ORNs for overlap between their terminals and LN and PN dendrites and, hence, in N-cad mutants, synapses between these elements are disrupted. The loss of glomerular structure observed in ALs innervated by *N-cad* mutant axons reflects not only their failure to converge but also the disorganization of their postsynaptic target dendrites. This may reflect a requirement for N-cad to promote the assembly of different neuronal processes into glomeruli or for N-cad to maintain these structures.

N-Cad Is Expressed on Developing ORN Axons and on Target Neuron Dendrites prior to Glomerulus Formation

As a first step toward assessing whether N-cad is required for formation or maintenance of glomeruli, we followed N-cad protein expression at different developmental stages. This was done using an antibody directed against the extracellular domain of N-cad (Figure 6). N-cad is expressed in ORNs projecting from the antenna (Figure 6A) and maxillary palp (Figure 6B). The AL was stained at various stages of pupal development. To correlate the expression of N-cad with developing ORN axons and PN dendrites, preparations were costained for CD8-GFP driven by the ORN- and PN-specific enhancer trap lines SG18.1-GAL4 (Figures 6C–6F) and GH146-GAL4 (Figures 6G–6J), respectively. These markers are expressed in most, but not all, ORNs and PNs early during pupal development. N-cad was observed in the developing AL neuropil at 15% pupal development (PD), prior to the arrival of ORN growth cones (Jefferis et al., 2004; T.H. and S.L.Z., unpublished data). This staining colocalized with PN dendrites but may also have included LN dendrites (the LN marker GH298 starts to be expressed after glomerulus formation). By 25% PD, N-cad was expressed on ORN axons within the nerve fiber layer surrounding the AL (Figures 6C, 6D, 6G, and 6H) and in the commissure (Figures 6C and 6D). Processes extended from the nerve fiber layer into the AL neuropil where they overlapped with PN dendrites (Figure 6D, inset). Glomerulus formation was visualized with ORN markers (green in Figures 6E and 6F), N-cad (red in Figures 6E, 6F, 6I, and 6J), and PN markers (green in Figures 6I and 6J). N-cad was strongly localized to ORN and PN processes from 25% PD through glomerulus formation (Figures 6D–6J). N-cad expression in glomeruli persisted into the adult (data not shown). In summary, the expression pattern of N-cad is consistent with a role in glomerulus formation, maintenance, or both.

N-cad Mutant ORN Axons Do Not Form Protoglomeruli

We sought to assess whether N-cad is required in ORNs for glomerulus formation or maintenance. As Or promoters are expressed after glomerulus formation, it was not possible to assess the role of N-cad in a large set of different subclasses of ORNs. As such, we turned to ORNs labeled at an early stage of development with the 72OK Gal4 driver expressing CD8-GFP (Acebes and Ferrus, 2001). This marker persists into the adult. It labels axons that converge onto two ventral-medial glomeruli, VM1 and VM4 (Figure 7A). As Figure 7A shows in a merged image of multiple optical sections, VM1 and VM4 appear to be direct neighbors. They are, however,

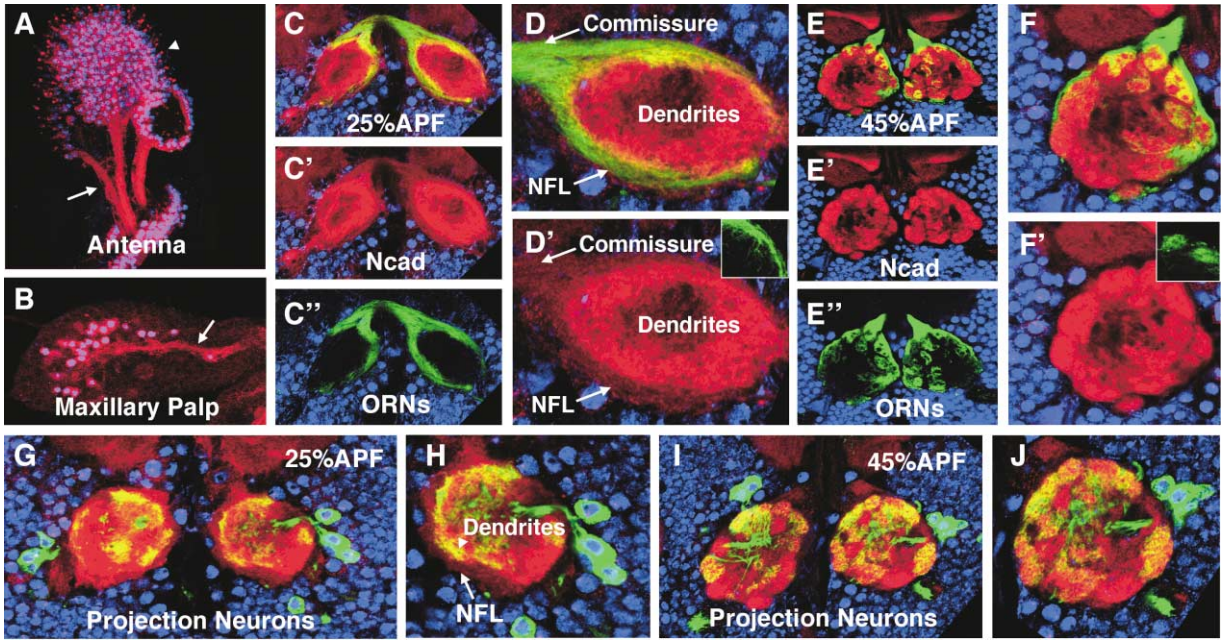

Figure 6. N-Cad Expression in the Developing Olfactory System

Anti-N-cad is shown in red. Markers for ORNs (SG18.1-Gal4; C–F) and PNs (GH146-Gal4; G–J) are shown in green. These markers are expressed in many, but not all, ORNs and PNs, respectively.

(A and B) N-cad expression in the peripheral olfactory organs, the antenna (A) and the maxillary palps (B) at about 40% pupal development (PD). N-cad is highly enriched in outgrowing ORN axons (arrow) projecting in three main fascicles in the antenna (A) as well as in axons of maxillary palp ORNs. (B) In addition, N-cad localizes to the sensory dendrites of ORNs (arrowhead in A).

(C–J) N-cad expression in the developing ALs during two different pupal stages, 25% PD (C, D, G, and H) and 45% PD (E, F, I, and J). Neuronal cell bodies stained with an antibody against the nuclear protein Elav are shown in blue. In the AL, N-cad colocalizes with ingrowing ORN axons as well as the dendrites of AL target neurons. (C and D) At about 25% PD, ORN axons leaving the antennal nerve project along the periphery of the AL toward the dorsal-medial commissural tract, where they cross the midline to innervate the contralateral AL. (D) Different levels of N-cad expression were detected in the dendritic field and on ORNs projecting in the NFL and commissure. (G and H) At 25% PD, the dendrites of different PNs (arrowhead) are largely separated from the NFL (arrow). Contact between ORNs and dendrites may take place within a narrow domain at the periphery of the dendritic field. (Inset in D′) Between 40% and 45% PD, glomeruli form, leading to the characteristic subdivision of the adult AL neuropil.

sufficiently distant along both the dorsoventral and anterioposterior axes to identify the individual target sites in both the developing and adult ALs. In *eyFLP*-induced clones, *N-cad* mutant 72OK axons spread out over the medial surface of the adult AL, a phenotype similar to that described above for Or22a and Or59c (Figure 7B, compare to Figure 2).

A time course of wild-type 72OK axonal targeting and subsequent VM1 glomerulus maturation from 25% to 45% PD is shown in Figures 7C–7F. Target dendrites express high levels of N-cad throughout pupal development and were used as postsynaptic markers; it is expressed at lower levels in ORN axons (see Figures 6C and 6D). At 25% PD, labeled ORNs projected along the ventral side of the AL and extended dorsally toward the commissure and into the contralateral lobe (Figure 7C). Small processes extending from the nerve fiber layer were seen in the ventral medial aspect of the developing lobe in an area roughly corresponding to the position to be occupied by the future VM1 target glomerulus. By 30% PD, a single tight cluster of 72OK fibers was seen (Figure 7D). Clusters became intensely stained by 35% PD (Figure 7E). While AL dendrites were in close proximity to ORN terminals at this early stage, they did not extensively mix with them, exhibiting an intense axonal GFP labeling. This early appearing structure is similar to so-called protoglomeruli described in various vertebrate and invertebrate species (Oland et al., 1990; Potter et al., 2001; Treloar et al., 1999). Protoglomeruli predominantly comprise knots of ORN terminal arbors and some PN and LN dendritic processes. By 45% PD, however, extensive intermingling of PN and ORN dendrites (Figure 7F) leads to glomerulus formation. This is seen as an apparent loosening of the protoglomerulus and yellow staining reflecting the intermixing of red and green labeled fibers.

Differences in *N-cad* mutant 72OK targeting were seen at early stages of AL development (Figures 7G–7J). As in wild-type, *N-cad* mutant 72OK axons selectively sent fine processes into a restricted region in the ventral medial AL (Figure 7G). Whereas by 30% PD, wild-type 72OK ORN processes converged to a tightly packed patch, *N-cad* mutant processes extended throughout a large region of the ventral medial AL without any sign of fiber convergence (Figure 7H). While *N-cad* mutant processes began to retract from the dendritic layer by 35% PD (Figure 7I), they did not form protoglomeruli. As development proceeded, mutant ORN processes segregated from dendrites and retracted to the surface of the AL (Figure 7J), a phenotype similar to that de-

scribed in the adult for all subclasses of ORNs studied (Figures 2 and 7B). These data indicate that N-cad is essential for glomerulus formation and acts in ORNs at an early step prior to protoglomerulus formation but after initial targeting to the appropriate region of the AL.

Discussion

A striking feature of olfactory system organization is the evolutionarily conserved arrangement of ORN terminals into an odortopic map. Here, ORNs expressing the same odorant receptors innervate common targets in a highly organized neuropilar structure, the glomerulus. In this paper, we demonstrated that mosaic animals in which N-cad was selectively removed from ORNs were largely devoid of glomeruli. Using a panel of ORN subclass-specific markers, we showed that ORN targeting to the appropriate region of the AL was not dependent upon N-cad. Developmental analysis revealed that N-cad is essential for protoglomerulus formation at an early stage of AL development. The analysis of N-cad thus supports the notion that targeting and glomerulus formation are distinct steps in constructing an olfactory sensory map.

N-Cad Is Required to Form Protoglomeruli

A series of studies in both vertebrate and invertebrates has underscored the key role played by ORNs in regulating glomerulus formation. Surgical ablation of the antennal primordium from the moth *Manduca sexta* results in the loss of glomerular structures (Tolbert and Sirianni, 1990), as does the genetic disruption of ORN development in *Drosophila* (Ang et al., 2003; Jhaveri and Rodrigues, 2002). Mouse ORNs form glomerular structures when forced to innervate ectopic sites in response to surgical or genetic ablation of the olfactory bulb (Graziadei and Kaplan, 1980; St John et al., 2003). These interactions may be instructive, as the pattern of sexually dimorphic glomeruli in gynandromorphs in the moth reflects the sex of the ORNs, not the sex of AL cells (Rossler et al., 1999). The molecular mechanisms that mediate the intrinsic capacity of ORNs to sort out in a subclass-specific manner are unknown. Our finding that genetically mosaic animals in which ORNs deficient in N-cad lack glomeruli provides further evidence that ORNs are essential for glomerular development and simultaneously identify a molecular component required in this process.

Developmental studies revealed a stereotyped pattern of glomerulus development in flies. ORNs send axons into the AL from early (~18 hr) through late (~100 hr) pupal development. Axons extend into the nerve fiber layer surrounding the incipient AL. Most ORNs project through the commissure to the contralateral AL. Studies with a panneuronal marker reveal that ORNs extend processes from the nerve fiber layer into the developing dendritic layer immediately after they reach the AL, on their way to the commissure. Using the 72OK marker, we demonstrated that axons of the same ORN subclass extend thin processes into a restricted area of the AL corresponding to the approximate position of the future glomerulus. These processes quickly grow and rapidly condense into a protoglomerulus.

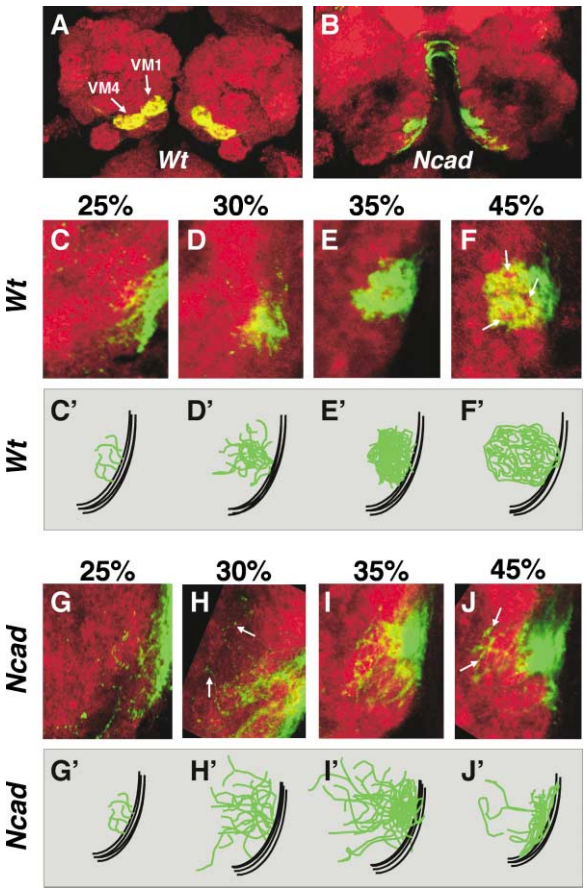

Figure 7. N-Cad Is Required in ORNs for Protoglomerulus Formation

The marker line 72OK highlights ORNs innervating VM1 and VM4 glomeruli both early during pupal development (C–J) and in the adult olfactory system (A and B). While there are many ORN subclass-specific markers in the adult, they are not expressed sufficiently early for developmental studies. (B) Targeting phenotype of 72OK-expressing *N-cad* mutant axons seen in the adult is similar to ORN classes shown in Figure 2. In eyflp-induced *N-cad* clones, terminals were spread over the medial surface of the AL. Development of wild-type (C–F and schematics in C′–F′) and *N-cad* mutant (G–J and schematics G′–J′) 72OK axons. Four stages of pupal development (PD) between 25% and 45% PD are shown. (C and C′) Between 20% and 25%, 72OK-positive axons were seen along the medial (right) surface of the AL projecting dorsally (up) and into the contralateral AL (not shown). In an area where the future VM1 glomerulus will form, 72OK axons extended short processes into the periphery of the dendritic field elaborated by AL target neurons. (D and D′) Axonal processes accumulated within a restricted region of the neuropil. (E and E′) At 35% PD, axon terminals formed a protoglomerulus, a tight discrete aggregate largely devoid of PN dendrites (see text). (F and F′) At 45%, ORN terminals intercalate with target dendrites (arrows). (G and G′) Initial targeting of processes of *N-cad* mutant axons to the ventral medial region of the AL at about 25% PD was similar to wild-type. (H and H′) In contrast to wild-type, *N-cad* mutant ORNs did not converge to a discrete spot at 30% PD; they extended profusely through the AL. A protoglomerulus did not form at 35% PD (I and I′). By 45% PD, most ORN processes retracted to the surface of the lobe (J and J′). Some processes remained in the neuropil in a region corresponding to the VM1 target area (arrows). AL dendrites were stained with anti-N-cad (see Figure 6 and text). Genotypes: (A, C–F) *eyFLP; 72OK-Gal4FRT40/Gal80 FRT40; UAS-mCD8GFP*; (B, G–J) *eyFLP; 72OK-Gal4 N-cad FRT40/ Gal80 FRT40; UAS-mCD8GFP*.

Protoglomeruli are largely peripheral to the mass of dendrites of AL projection neurons. Glomerulus formation ensues as ORN processes and PN dendrites intermingle. The sequence of events leading to glomerulus formation is in many ways phylogenetically conserved (Kasowski et al., 1999; Klenoff and Greer, 1998; Oland et al., 1990; Treloar et al., 1999). It is important to note, however, that the dynamics of glomerulus formation differ between different subclasses of mouse ORNs (Potter et al., 2001; Royal and Key, 1999; Treloar et al., 2002; Zheng et al., 2000). Nevertheless, in both vertebrates and invertebrates, the formation of protoglomeruli largely comprising the processes of ORNs occurs prior to extensive intercalation with dendrites of target neurons.

N-cad mutant ORNs do not form protoglomeruli. 72OK ORNs lacking *N-cad* extend processes into the appropriate region of the lobe. In striking contrast to wild-type, however, rather than condensing into protoglomeruli at 35% PD, ORN axons extend farther throughout the ventral medial region of the AL before retracting back to the surface of the neuropil. They remain segregated from the dendrites of target neurons. While markers for other subsets of ORNs early in development are not available, it is likely that the process visualized with 72OK will extend to other ORNs, as developmental analysis with a panneuronal marker reveals a widespread failure of protoglomerulus formation (data not shown). Furthermore, adult *N-cad* mutant ORN processes terminate on the surface of the lobe in close proximity to the position of the glomerulus in a wild-type animal. These studies establish N-cad as a key regulator of the cellular interactions underlying the formation of protoglomeruli.

N-Cad Promotes Subclass-Specific Convergence of ORNs

The subclass-specific convergence of ORN axons reflects specific interactions between ORN terminals within the target region. In both the mouse and fly, the cell bodies of different ORN subclasses are scattered throughout the nasal epithelium and the antenna, respectively. ORN axons do not segregate into subclass-specific fascicles as they project to the target (Treloar et al., 2002; T.H. and S.L.Z., unpublished observation). Association between axon terminals takes place within the target region itself. That different ORNs show affinity for fibers of the same subclass is supported by studies in both organisms. In the mouse *extratoes* mutant, the olfactory bulb fails to form. ORNs terminate instead in a fibrocellular mass lacking PNs and only a small number of LNs (St John et al., 2003). Despite the lack of target neurons, P2 neurons sort out into a glomerular-like structure. Additional studies by Mombaerts and colleagues (Vassalli et al., 2002) indicate that ORNs expressing the same odorant receptors show selective affinity. Mice expressing odorant receptor transgenes in ORNs that lie in inappropriate epithelial zones form ectopic glomeruli in regions of the olfactory bulb distinct from those formed by ORNs expressing the endogenous receptor. In some cases, however, axons from ORNs expressing the endogenous receptors are recruited into these ectopic glomeruli. We reached a similar conclusion in previous studies exploring targeting defects in ORNs mutant for *Dscam* (Hummel et al., 2003). ORNs lacking *Dscam* target to inappropriate regions of the AL; indeed, several subclasses of ORNs terminate in the wrong ganglion in these mutants. Nevertheless, ORNs of the same subclass sort out from fibers of other ORN classes to form separate, often adjacent, ectopic glomeruli.

The homophilic cell adhesion activity of N-cad (Iwai et al., 1997) supports a simple model for its function in the developing fly olfactory system. Here N-cad acts to promote interactions between ORN terminals of the same subclass. It is likely that this interaction is largely permissive in nature as N-cad is widely expressed, and removal of N-cad from ORNs leads to a similar axonal phenotype for all 10 ORN subclasses tested. In contrast to the permissive function for N-cad in protoglomerulus formation in flies, odorant receptors appear to play an instructive role in this process in vertebrates. Genetic and expression studies indicate that odorant receptors do not play a role in ORN convergence in flies (Dobritsa et al., 2003), although it remains possible that a subset of these receptors not yet tested will, as in vertebrates, serve this function.

Could N-cad play an instructive role in sorting? As ORNs target to the appropriate region of the lobe, the sorting problem is reduced to sorting among a small number of different ORN subclasses within a local region. Modulation of N-cad activity in different classes may provide sufficient specificity for sorting. Indeed, cells in culture expressing different levels of cadherins sort out from one another (Steinberg and Takeichi, 1994). As panneuronal expression of a single form of N-cad in ORNs rescues the *N-cad* mutant targeting phenotypes, it is unlikely that different levels of N-cad protein specified at the level of transcription or different isoforms produced by alternative splicing underlie specific sorting. Presumably, other cell surface components in fly ORNs mediate subclass-specific sorting to protoglomeruli modulating the core homophilic cell adhesion activity of N-cad.

N-cad may not mediate adhesion between ORNs, but rather may promote interactions between ORNs and target dendrites. In the fly visual system, for instance, we previously showed that N-cad is required in R7 photoreceptor neurons to select the appropriate target region (Lee et al., 2001). Genetic mosaic studies support the view that this reflects interactions between R7 growth cones and their targets rather than between R7 neurons and other photoreceptor neurons (A. Nern and S.L.Z., unpublished data). Since N-cad is expressed on both ORNs and target neurons as ORNs enter the target region, it is expressed at the right place and time to mediate interactions between them. Recent studies reported in this issue of *Neuron* by Zhu and Luo (2004), however, indicate that glomerulus formation does not require N-cad in PN dendrites. N-cad may also play a subsequent role in mediating interactions between ORNs and targets, but it will be necessary to assess glomerulus development in animals in which N-cad is removed after formation of protoglomeruli to critically address this issue.

Interactions between Axonal Processes May Be a Common Mechanism Regulating Connection Specificity

While adhesion between ORN terminals has emerged as a common theme from work in both vertebrate and invertebrate systems, specific interactions between axons within the target region may be a more widespread phenomenon. Indeed, in the *Drosophila* visual system, the exquisite target specificity of different subclasses of R1-R6 photoreceptor axons relies upon interactions between them (Clandinin and Zipursky, 2000). In wild-type animals, R1-R6 axons from a single ommatidium project away from each other to a distinct set of targets. We previously demonstrated that this requires N-cad (Lee et al., 2001) and proposed that N-cad mediates adhesive interactions between R cells and their targets. While biochemical studies support an adhesive function for classical cadherins, the *N-cad* phenotypes in R1-R6 and ORNs are also consistent with a repellent function. N-cad on R cell axons may promote repulsive interactions between them rather than mediating adhesion between R cell axons and target cells. In the olfactory system, N-cad may promote repulsive interactions between different classes of ORNs, thereby leading to their segregation rather than promoting interactions between axon terminals of the same class. That N-cad may mediate repellent interactions between neurites is supported by elegant genetic analysis by Zhu and Luo (2004) of a requirement for N-cad in mediating interactions between PN dendrites. We previously proposed that repellent interactions between R8 axons play a crucial role in elaborating a precise topographic map in the fly visual system and that the protocadherin Flamingo serves this function (Lee et al., 2001). Whether interactions between afferents are adhesive or repulsive, or indeed whether they interact in a more complex and instructive fashion, these studies raise the important issue that afferent interactions may play crucial and hitherto poorly appreciated roles in the elaboration of specific patterns of synaptic connectivity.

N-Cad and Dscam Mediate Distinct Steps in Targeting of ORNs

The molecular mechanisms underlying the formation of an odortopic map presents a complex problem in cellular recognition (Brunjes and Greer, 2003; Lin and Ngai, 1999; Mombaerts, 2001). A major advance in this field was the discovery that odorant receptors in the mouse play an instructive role in ORN targeting (Chess, 2000; Hellman and Chess, 2002). Given the striking conservation in the cellular organization in the olfactory system of the mouse and fly, it is surprising that fly odorant receptors do not serve this key targeting function. Target specificity in this system must rely on other cellular recognition mechanisms. In previous work, we demonstrated that the Ig superfamily protein Dscam plays a crucial role in targeting some, but not all, ORNs (Hummel et al., 2003). In the absence of Dscam, some subclasses of ORNs target to inappropriate regions of the AL, where they form ectopic glomeruli. Hence, Dscam contributes to target specificity, whereas N-cad acts at a later step to promote the formation of protoglomeruli. We anticipate that further studies on N-cad and Dscam, as well as other cell surface and signaling proteins identified in ongoing genetic screens for targeting mutants in the olfactory system, will lead to a detailed molecular understanding of the cellular interactions underlying the exquisite specificity of neuronal connections in the fly olfactory system.

Experimental Procedures

Genetics

Fly stocks were maintained in standard medium at 22°C unless stated otherwise. Four different *N-cad* alleles were analyzed, *N-cad^{M19}* (Iwai et al., 1997), *N-cad^{I405}* (Clandinin and Zipursky, 2000), *N-cad^{B11}* (Lee et al., 2001), and *N-cad^{4C}* (Lee et al., 2001). All *N-cad* alleles lead to similar axonal defects in MARCM-induced ORN clones.

Markers for Different ORN Subclasses and AL Neurons

To label a subset of ORNs, we used the following promoters fused to Gal4: Or22a, Or23a, Or46a, Or47a, Or47b (Vosshall et al., 2000), Or59c, and Or71c (Hummel et al., 2003). Axons innervating the V glomerulus were detected using the enhancer trap insertion GH298-Gal4 (Stocker et al., 1997). The reporters to visualize axons and synaptic terminals were UAS-mCD8-GFP (Lee and Luo, 1999), UAS>CD2>CD8-GFP (Wong et al., 2002), and UAS-N-synaptobrevin-GFP (Estes et al., 2000). To visualize all ORNs in mosaics, the enhancer trap line Gal4-C155 (elav-Gal4; Lin and Goodman, 1994) was used. SG18.1-Gal4 is preferentially expressed in early projecting ORNs (Jhaveri and Rodrigues, 2002). In addition to ORNs innervating the V glomerulus, the GH298-Gal4 line is expressed in LNs (Stocker et al., 1997). Projection neurons were visualized with the enhancer trap line GH146-Gal4 (Stocker et al., 1997). For simultaneous visualization of target neurons and ORN terminals, the N-synaptobrevin-GFP was directly expressed under OR22a promotor control (A.I. Domingos and L.B. Vosshall, personal communication).

Genetic Mosaics

The majority of the genetic mosaics were generated using the MARCM system (Lee and Luo, 1999) with various Gal4 drivers (see previous section) and *TubP-Gal80 FTR40*. For large clones in the antenna and maxillary palps, an *eyFLP* insertion on the X chromosome was used (Newsome et al., 2000). For small clones and single-cell analysis, a *hsp70-Flp* transgene on the X chromosome was used (Golic and Lindquist, 1989). To visualize all ORNs, mosaics were generated in flies of the following genotype: *eyFLP; FRT40/Gal80 FRT40; elav-Gal4 UAS-mCD8GFP* and *eyFLP; N-cad FRT40/Gal80 FRT40; elav-Gal4 UAS-mCD8GFP*. To visualize ORN subclasses, mosaics were generated in flies of the following genotype: *eyFLP*; *FRT40/Gal80 FRT40; Or-Gal4 UAS-sybGFP* and *eyFLP; N-cad FRT40/Gal80 FRT40; Or-Gal4 UAS-sybGFP*. To increase the fraction of *N-cad* mutant ORNs, we generated *N-cad* mutant clones in a genetic background in which heterozygous cells were also heterozygous for a *cycE* mutation; after mitotic recombination, cells homozygous for the wild-type allele of *N-cad* were homozygous for *cycE*. Cells homozygous for the *cycE* mutation cannot proliferate, and *cycE/+* cells compete poorly for growth with cells homozygous for *N-cad* mutant cells carrying two wild-type copies of *cycE*. As recombination promoted by *eyFLP* occurs multiple times in a given lineage, the inclusion of a *cycE* mutation linked to the wild-type *N-cad* allele markedly increases the proportion of disc cells homozygous for *N-cad*. Genotype used: *eyFLP; Ncad FRT40/cycE FRT40; Or-Gal4 UAS-sybGFP*. Single-cell clones were obtained by heat shocking late third instar larvae (30 min at 37°C) of the following genotypes: *hs-Flp*; *FRT40/Gal80 FRT40; Or22a-Gal4 UAS-mCD8GFP* and *hs-Flp*; *N-cad FRT40/Gal80 FRT40; Or22a-Gal4 UAS-mCD8GFP*. In rescue experiments, the phenotype of the following to genotypes were compared: *eyFLP elav-Gal4/+ ; Or22a-sybGFP N-cad FRT40/Gal80 FRT40* and *eyFLP elav-Gal4/ UAS-N-cad ; Or22a-sybGFP N-cad FRT40/Gal80 FRT40*. To visualize ORN terminals and target cell dendrites, we used the following genotype: *eyFLP; Or22a-sybGFP FRT40/cycE FRT40; GH298-Gal4 UAS-LacZ*

and *eyFLP; Or22a-sybGFP N-cad FRT40/cycE FRT40; GH298-Ga4 UAS-LacZ* and *eyflp/hsflp; GH146-Gal4 N-cad FRT40/cycE FRT40; UAS>CD2>CD8-GFP*. Developmental studies with the marker 72OK were performed using pupae of the following genotypes: *eyFLP; 72OK-Gal4FRT40/Gal80 FRT40; UAS-mCD8GFP* and *eyFLP; 72OK-Gal4 Ncad FRT40/Gal80 FRT40; UAS-mCD8GFP*.

Immunohistology

Primary antibodies used for immunohistochemistry were rat anti-N-cadherin extracellular domain (Iwai et al., 1997), rabbit anti-GFP (Molecular Probes) and nc82 (Stortkuhl et al., 1994), and mouse anti-ELAV (DSHB). Secondary antibodies used were goat anti-rabbit F(ab)' fragment coupled to Alexa-488 (Molecular Probes), goat anti-mouse F(ab)' fragment coupled to Alexa-568 (Molecular Probes), goat anti-rat F(ab)' fragment coupled to Alexa-568 (Molecular Probes), and goat anti-mouse F(ab)' fragment coupled to Alexa-648 (Molecular Probes). For general nuclear staining, TOTO-3 (Molecular Probes) was used.

Immunostaining of brains of adult flies and pupae were carried out essentially as described in Van Vactor et al. (1991), with the following exceptions: (1) adult brains were fixed in 2% PFA for 90 min, and (2) for the dissection of the pupal brains, the pupal cases were open, 2% PFA was added, and the brains were allowed to fix for 10 min before further dissection in 2% PFA. The overall time of fixation in 2% PFA was 90 min. Fluorescent samples were analyzed using a Bio-Rad MRC1024 confocal microscope.

Acknowledgments

We thank R. Stocker, L. Vosshall, R. Axel, K.F. Stortkuhl, and T. Uemura for fly stocks and antibodies and members of the Zipursky and Hummel laboratories, C. Klaembt, and K. Schimmelpfeng for comments on the manuscript and discussion. We particularly wish to thank Haitao Zhu and Liqun Luo for sharing unpublished results and for discussions and comments on the manuscript. T.H. was supported by an HFSP Long-Term Fellowship and the Deutsche Forschungsgemeinschaft (SFB 629 B04). S.L.Z. is an investigator of the Howard Hughes Medical Institute.

Received: December 15, 2003
Revised: February 13, 2004
Accepted: March 4, 2004
Published: April 7, 2004

References

Acebes, A., and Ferrus, A. (2001). Increasing the number of synapses modifies olfactory perception in *Drosophila*. J. Neurosci. *21*, 6264–6273.

Ang, L.H., Kim, J., Stepensky, V., and Hing, H. (2003). Dock and Pak regulate olfactory axon pathfinding in *Drosophila*. Development *130*, 1307–1316.

Brunjes, P.C., and Greer, C.A. (2003). Progress and directions in olfactory development. Neuron *38*, 371–374.

Chess, A. (2000). Odorant receptors: axon contact-mediated diversity. Curr. Biol. *10*, R152–R154.

Clandinin, T., and Zipursky, S.L. (2000). Afferent growth cone interactions control synaptic specificity in the *Drosophila* visual system. Neuron *28*, 427–436.

Dobritsa, A.A., van der Goes van Naters, W., Warr, C.G., Steinbrecht, R.A., and Carlson, J.R. (2003). Integrating the molecular and cellular basis of odor coding in the *Drosophila* antenna. Neuron *37*, 827–841.

Ebrahimi, F.A., and Chess, A. (2000). Olfactory neurons are interdependent in maintaining axonal projections. Curr. Biol. *10*, 219–222.

Elmore, T., and Smith, D.P. (2001). Putative *Drosophila* odor receptor OR43b localizes to dendrites of olfactory neurons. Insect Biochem. Mol. Biol. *31*, 791–798.

Elmore, T., Ignell, R., Carlson, J.R., and Smith, D.P. (2003). Targeted mutation of a *Drosophila* odor receptor defines receptor requirement in a novel class of sensillum. J. Neurosci. *23*, 9906–9912.

Estes, P.S., Ho, G.L., Narayanan, R., and Ramaswami, M. (2000). Synaptic localization and restricted diffusion of a *Drosophila* neuronal synaptobrevin–green fluorescent protein chimera in vivo. J. Neurogenet. *13*, 233–255.

Gao, Q., Yuan, B., and Chess, A. (2000). Convergent projections of *Drosophila* olfactory neurons to specific glomeruli in the antennal lobe. Nat. Neurosci. *3*, 780–785.

Goheen, B.L., Kott, J.N., Anderson, N.L., Kim, A., and Westrum, L.E. (1995). Host primary olfactory axons make synaptic contacts in a transplanted olfactory bulb. J. Comp. Neurol. *352*, 203–212.

Golic, K.G., and Lindquist, S. (1989). The FLP recombinase of yeast catalyzes site-specific recombination in the *Drosophila* genome. Cell *59*, 499–509.

Goodhill, G.J., and Richards, L.J. (1999). Retinotectal maps: molecules, models and misplaced data. Trends Neurosci. *22*, 529–534.

Graziadei, P.P., and Kaplan, M.S. (1980). Regrowth of olfactory sensory axons into transplanted neural tissue. 1. Development of connections with the occipital cortex. Brain Res. *201*, 39–44.

Graziadei, P.P., and Monti Graziadei, G.A. (1986). Principles of organization of the vertebrate olfactory glomerulus: an hypothesis. Neuroscience *19*, 1025–1035.

Hellman, A., and Chess, A. (2002). Olfactory axons: a remarkable convergence. Curr. Biol. *12*, R849–R851.

Hildebrand, J.G., and Shepherd, G.M. (1997). Mechanisms of olfactory discrimination: converging evidence for common principles across phyla. Annu. Rev. Neurosci. *20*, 595–631.

Hummel, T., Vasconcelos, M.L., Clemens, J.C., Fishilevich, Y., Vosshall, L.B., and Zipursky, S.L. (2003). Axonal targeting of olfactory receptor neurons in *Drosophila* is controlled by Dscam. Neuron *37*, 221–231.

Iwai, Y., Usui, T., Hirano, S., Steward, R., Takeichi, M., and Uemura, T. (1997). Axon patterning requires DN-cadherin, a novel neuronal adhesion receptor, in the *Drosophila* embryonic CNS. Neuron *19*, 77–89.

Jefferis, G.S., Marin, E.C., Stocker, R.F., and Luo, L. (2001). Target neuron prespecification in the olfactory map of *Drosophila*. Nature *414*, 204–208.

Jefferis, G.S., Vyas, R.M., Berdnik, D., Ramaekers, A., Stocker, R.F., Tanaka, N.K., Ito, K., and Luo, L. (2004). Developmental origin of wiring specificity in the olfactory system of *Drosophila*. Development *131*, 117–130.

Jhaveri, D., and Rodrigues, V. (2002). Sensory neurons of the Atonal lineage pioneer the formation of glomeruli within the adult *Drosophila* olfactory lobe. Development *129*, 1251–1260.

Kasowski, H.J., Kim, H., and Greer, C.A. (1999). Compartmental organization of the olfactory bulb glomerulus. J. Comp. Neurol. *407*, 261–274.

Kent, K.S., Oland, L.A., and Hildebrand, J.G. (1999). Development of the labial pit organ glomerulus in the antennal lobe of the moth *Manduca sexta*: the role of afferent projections in the formation of identifiable olfactory glomeruli. J. Neurobiol. *40*, 28–44.

Klenoff, J.R., and Greer, C.A. (1998). Postnatal development of olfactory receptor cell axonal arbors. J. Comp. Neurol. *390*, 256–267.

Komiyama, T., Johnson, W.A., Luo, L., and Jefferis, G.S. (2003). From lineage to wiring specificity. POU domain transcription factors control precise connections of *Drosophila* olfactory projection neurons. Cell *112*, 157–167.

Laissue, P.P., Reiter, C., Hiesinger, P.R., Halter, S., Fischbach, K.F., and Stocker, R.F. (1999). Three-dimensional reconstruction of the antennal lobe in *Drosophila melanogaster*. J. Comp. Neurol. *405*, 543–552.

Lee, T., and Luo, L. (1999). Mosaic analysis with a repressible cell marker for studies of gene function in neuronal morphogenesis. Neuron *22*, 451–461.

Lee, C.H., Herman, T., Clandinin, T.R., Lee, R., and Zipursky, S.L. (2001). N-cadherin regulates target specificity in the *Drosophila* visual system. Neuron *30*, 437–450.

Lin, D.M., and Goodman, C.S. (1994). Ectopic and increased expression of Fasciclin II alters motoneuron growth cone guidance. Neuron *13*, 507–523.

Lin, D.M., and Ngai, J. (1999). Development of the vertebrate main olfactory system. Curr. Opin. Neurobiol. *9*, 74–78.

Mombaerts, P. (2001). How smell develops. Nat. Neurosci. *4* (*Suppl*), 1192–1198.

Mombaerts, P., Wang, F., Dulac, C., Chao, S.K., Nemes, A., Mendelsohn, M., Edmondson, J., and Axel, R. (1996). Visualizing an olfactory sensory map. Cell *87*, 675–686.

Newsome, T.P., Asling, B., and Dickson, B.J. (2000). Analysis of *Drosophila* photoreceptor axon guidance in eye-specific mosaics. Development *127*, 851–860.

Oland, L.A., and Tolbert, L.P. (1996). Multiple factors shape development of olfactory glomeruli: insights from an insect model system. J. Neurobiol. *30*, 92–109.

Oland, L.A., and Tolbert, L.P. (1998). Glomerulus development in the absence of a set of mitral-like neurons in the insect olfactory lobe. J. Neurobiol. *36*, 41–52.

Oland, L.A., Orr, G., and Tolbert, L.P. (1990). Construction of a protoglomerular template by olfactory axons initiates the formation of olfactory glomeruli in the insect brain. J. Neurosci. *10*, 2096–2112.

Potter, S.M., Zheng, C., Koos, D.S., Feinstein, P., Fraser, S.E., and Mombaerts, P. (2001). Structure and emergence of specific olfactory glomeruli in the mouse. J. Neurosci. *21*, 9713–9723.

Ressler, K.J., Sullivan, S.L., and Buck, L.B. (1994). Information coding in the olfactory system: evidence for a stereotyped and highly organized epitope map in the olfactory bulb. Cell *79*, 1245–1255.

Rossler, W., Randolph, P.W., Tolbert, L.P., and Hildebrand, J.G. (1999). Axons of olfactory receptor cells of transsexually grafted antennae induce development of sexually dimorphic glomeruli in *Manduca sexta*. J. Neurobiol. *38*, 521–541.

Royal, S.J., and Key, B. (1999). Development of P2 olfactory glomeruli in P2-internal ribosome entry site-tau-LacZ transgenic mice. J. Neurosci. *19*, 9856–9864.

Royal, S.J., Gambello, M.J., Wynshaw-Boris, A., Key, B., and Clarris, H.J. (2002). Laminar disorganisation of mitral cells in the olfactory bulb does not affect topographic targeting of primary olfactory axons. Brain Res. *932*, 1–9.

St John, J.A., Clarris, H.J., McKeown, S., Royal, S., and Key, B. (2003). Sorting and convergence of primary olfactory axons are independent of the olfactory bulb. J. Comp. Neurol. *464*, 131–140.

Steinberg, M.S., and Takeichi, M. (1994). Experimental specification of cell sorting, tissue spreading, and specific spatial patterning by quantitative differences in cadherin expression. Proc. Natl. Acad. Sci. USA *91*, 206–209.

Stocker, R.F. (1994). The organization of the chemosensory system in *Drosophila melanogaster*: a review. Cell Tissue Res. *275*, 3–26.

Stocker, R.F., Lienhard, M.C., Borst, A., and Fischbach, K.F. (1990). Neuronal architecture of the antennal lobe in *Drosophila melanogaster*. Cell Tissue Res. *262*, 9–34.

Stocker, R.F., Heimbeck, G., Gendre, N., and de Belle, J.S. (1997). Neuroblast ablation in *Drosophila* P[GAL4] lines reveals origins of olfactory interneurons. J. Neurobiol. *32*, 443–456.

Stowers, R.S., and Schwarz, T.L. (1999). A genetic method for generating *Drosophila* eyes composed exclusively of mitotic clones of a single genotype. Genetics *152*, 1631–1639.

Stortkuhl, K.F., Hofbauer, A., Keller, V., Gendre, N., and Stocker, R.F. (1994). Analysis of immunocytochemical staining patterns in the antennal system of *Drosophila melanogaster*. Cell Tissue Res. *275*, 27–38.

Strausfeld, N.J., and Hildebrand, J.G. (1999). Olfactory systems: common design, uncommon origins? Curr. Opin. Neurobiol. *9*, 634–639.

Sullivan, S.L., Ressler, K.J., and Buck, L.B. (1995). Spatial patterning and information coding in the olfactory system. Curr. Opin. Genet. Dev. *5*, 516–523.

Tolbert, L.P., and Sirianni, P.A. (1990). Requirement for olfactory axons in the induction and stabilization of olfactory glomeruli in an insect. J. Comp. Neurol. *298*, 69–82.

Treloar, H.B., Purcell, A.L., and Greer, C.A. (1999). Glomerular formation in the developing rat olfactory bulb. J. Comp. Neurol. *413*, 289–304.

Treloar, H.B., Feinstein, P., Mombaerts, P., and Greer, C.A. (2002). Specificity of glomerular targeting by olfactory sensory axons. J. Neurosci. *22*, 2469–2477.

Valverde, F., Santacana, M., and Heredia, M. (1992). Formation of an olfactory glomerulus: morphological aspects of development and organization. Neuroscience *49*, 255–275.

Van Vactor, D.L., Jr., Cagan, R.L., Kramer, H., and Zipursky, S.L. (1991). Induction in the developing compound eye of *Drosophila*: multiple mechanisms restrict R7 induction to a single retinal precursor cell. Cell *61*, 1145–1155.

Vassalli, A., Rothman, A., Feinstein, P., Zapotocky, M., and Mombaerts, P. (2002). Minigenes impart odorant receptor-specific axon guidance in the olfactory bulb. Neuron *35*, 681–696.

Vosshall, L.B., Wong, A.M., and Axel, R. (2000). An olfactory sensory map in the fly brain. Cell *102*, 147–159.

Wang, F., Nemes, A., Mendelsohn, M., and Axel, R. (1998). Odorant receptors govern the formation of a precise topographic map. Cell *93*, 47–60.

Wilkinson, D.G. (2000). Eph receptors and ephrins: regulators of guidance and assembly. Int. Rev. Cytol. *196*, 177–244.

Wong, A.M., Wang, J.W., and Axel, R. (2002). Spatial representation of the glomerular map in the *Drosophila* protocerebrum. Cell *109*, 229–241.

Zheng, C., Feinstein, P., Bozza, T., Rodriguez, I., and Mombaerts, P. (2000). Peripheral olfactory projections are differentially affected in mice deficient in a cyclic nucleotide-gated channel subunit. Neuron *26*, 81–91.

Zhu, H., and Luo, L. (2004). Diverse functions of N-cadherin in dendritic and axonal terminal arborization of olfactory projections neurons. Neuron *42*, this issue, 63–75.